Article:
Xu, S, Sun, J, Weng, L et al. (5 more authors) (2018) In-situ friction and wear responses of WS_2 films to space environment: Vacuum and atomic oxygen. Applied Surface Science, 447. pp. 368-373. ISSN 0169-4332

https://doi.org/10.1016/j.apsusc.2018.04.012

Highlights

► Dense pure WS_2 film with high wear resistance in vacuum was made successfully;

► The response of WS_2 film to space environments has been investigated by in-situ method;

►Wear life of film declined sharply as switching vacuum to atomic oxygen condition;

►High friction and wear mechanism induced by atomic oxygen was discussed systematically.

Graphical Abstract

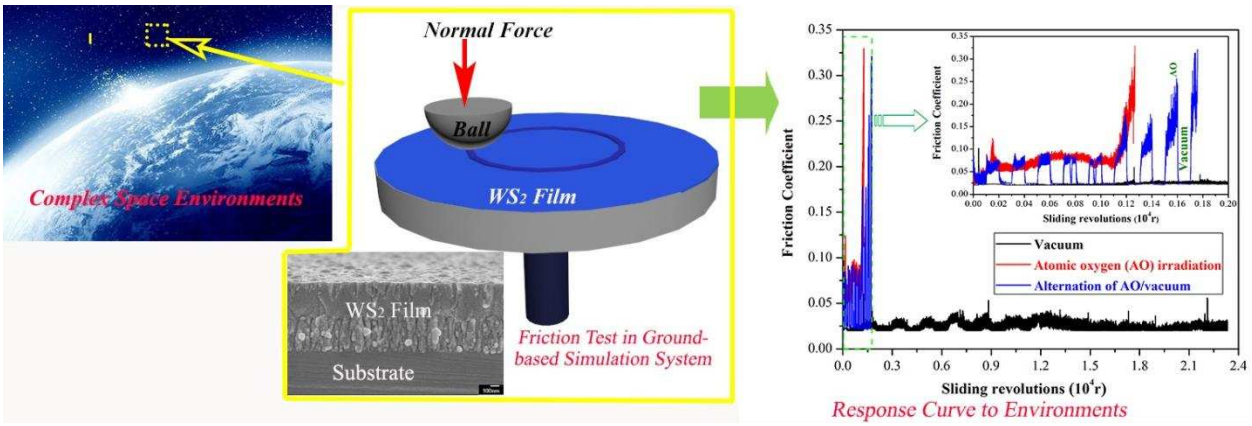

In-situ friction and wear responses of WS_2 films to space environment: vacuum and atomic oxygen

Shusheng Xu[a,b], Jiayi Sun[a], Lijun Weng[a], Yong Hua[b], Weimin Liu[a], Anne Neville[b], Ming Hu[a,**], Xiaoming Gao[a,*]

[a] State Key Laboratory of Solid Lubrication, Lanzhou Institute of Chemical Physics, Chinese Academy of Sciences, Lanzhou 730000, P.R. China

[b]Institute of Functional Surfaces, School of Mechanical Engineering, University of Leeds, Leeds, LS2 9JT, UK

*Corresponding author. gaoxm@licp.cas.cn (Xiaoming Gao); hum413@licp.cas.cn (Ming Hu)

Abstract

The Friction and wear behavior of both sputtered WS_2 films with loose or dense microstructures were investigated in vacuum, atomic oxygen (AO) and vacuum/AO irradiation alternate environments. The loose microstructure of pure WS_2 film composed of columnar platelets and vertical pores and the dense microstructure showed high compactness. The results revealed that the WS_2 films exhibited a periodic fluctuant friction coefficient and high wear under the synchronization action of AO irradiation and friction (in-situ condition). The in-situ results also indicated significantly difference from that of conventional ex-situ methods. As the friction environments were switched from vacuum to in-situ AO, the friction coefficients of the two types of films increased from 0.03 to 0.07 and the wear life of them declined identically to a small value of ~1.1×10^3 cycles, although the wear life of loose WS_2 film was up to 1.7×10^4 cycles and that of the dense film was longer than 2.3×10^4 cycles in vacuum. The friction and wear behavior did not depend on the film compactness but the anti-oxidation ability of WS_2 itself. For in-situ AO irradiation condition, the high friction resulted from the formation of oxidation product (WO_3) by AO and its delamination by frictional interaction was responsible for high wear.

Keywords: In-situ; Atomic oxygen; WS_2 films; Friction; Wear

1. Introduction

With the rapid development of space technology, the required service lives of spacecrafts are getting much longer so that the reliability has become increasingly important. The space environment remains a major cause of various anomalies and even emergent failures for different spacecrafts [1]. The atomic oxygen (AO) is the dominant environmental species and mainly negative factor in low earth orbit (LEO, 200-1000 km altitudes) cosmic environment, where the AO exhibited high flux density (~10^{13}-10^{15} atoms·cm^{-2}·s^{-1}) and kinetic energy (~5 eV) on exposed surfaces due to the spacecraft's high orbital velocity up to ~8 km/s [2]. Previous studies and space mission reports [3-5] revealed that many materials would be oxidized and eroded by the AO irradiation and cosmic environment exposure, and hence much more attentions should be paid to the response behavior of spacecraft materials to the AO environment.

Solid lubricants are widely utilized in the space technology field owing to their outstanding advantages as compared to conventional oils and greases [6], and the sputtered transition-metal-disulfides (TMDs, such as MoS_2 and WS_2) films might be the optimal solid lubricants. Two typical approaches (referred to as ex-situ and in-situ) have been employed to investigate the effects of atomic oxygen on the chemical, structural and property evolution of solid lubricants [7, 8]. In the ex-situ method, the TMDs films were irradiated by AO for different durations in the ground simulation system or real space flight experiments in LEO. Afterwards, the structure, chemical composition and properties of irradiated films were analyzed and investigated as compared to the original films. It is generally confirmed that the MoS_2 films were oxidized to MoO_3 by AO, but this was restricted to the surface layer owing to the protective function of the dense oxidation surface layer [9-16]. Reasonably, the ex-situ AO irradiation effect on the tribological properties of MoS_2 based films only exhibited a significant increase of friction coefficient in the initial stage of friction process [15, 16]. The slightly negative influence on the lubrication action of MoS_2 films would never be a potential danger to the spacecraft. Actually, it must be noticed that the abovementioned response of friction behavior to the ex-situ AO irradiation could merely represent ideal one-shot movement of the degraded MoS_2 film, but it diverges far from the practical multi-cycle working mode. In the in-situ method, the evolution of structure and property changes of the materials is directly investigated in actual or simulated working conditions [8]. There is no doubt that this in-situ way is much more accurate and reliable than ex-situ measurement to reveal the real-time friction and wear behavior of solid lubricants under the AO irradiation in LEO environments. Tagawa et al. [8] simply found that the friction behavior of MoS_2 films under in-situ AO irradiation was different from that of ex-situ irradiation. Krick et al. [17] gave an outline of in-situ frictional experiments of MoS_2 based films in the space environment, where eight pin-on-disk tribometers were directly exposed to the LEO environment (MISSE, Materials on the International Space Station Experiments Platform), but the expected results were not reported in detail. Nevertheless, the most research works of the effect of AO irradiation have been implemented by the ex-situ method and it also mainly focused on traditional MoS_2 films. Thus, it is very important to well understand the friction and wear behaviors of TMDs films using the in-situ method to avoid possible lubrication failures and ensure the high reliability of LEO-serviced spacecrafts.

The WS_2 film, a typical family member of the TMDs that possesses higher thermal stability than the traditional MoS_2, was prepared by vacuum sputter technology in this work. The tribological properties were investigated in the vacuum, AO irradiation and vacuum/AO irradiation alternate environments, respectively. The friction and wear behavior of these WS_2 films are characterized in the in-situ conditions. In addition, it

should be noted that the WS_2 composite films were not taken into consideration here in order to avoid some concerns relating to the effects of dopants on the masking response of the WS_2 phase to environment, although the WS_2 composite films normally showed better tribological properties [18, 19]. Herein, considering that the structural densification was the main positive factor for better tribological properties of the composite films [20], the WS_2 films with both loose and dense microstructures were designed and investigated systematically.

2. Experimental detail

2.1 Film deposition

The WS_2 films were deposited on Si (100) wafers using a sputtering system in argon plasma atmosphere. The WS_2 target (Φ 80mm, 99.99 wt.%) was utilized as the cathode of radio frequency power supply (13.56 MHz, COMDEL, Gloucester, MA, USA). Prior to deposition, the wafers were ultrasonically cleaned in acetone and then they were put into the vacuum chamber and fixed on the sample holder. As the vacuum chamber was evacuated to a base pressure lower than 8.0×10^{-4} Pa, the substrates' surface was etched in argon plasma for 10 minutes to eliminate possible contaminants. Afterwards, a Ti interlayer with a thickness of ~30 nm was deposited on the substrates to improve the film-substrate adhesion at argon pressure of 1.0 Pa, radio frequency power of 300 W and substrate bias voltage of -100 V. After that, the WS_2 film was deposited at radio frequency power of 400 W and bias voltage of -100 V. Both the argon pressures of 1.2 Pa and 2.5 Pa were used to construct dense and loose film microstructures, respectively. The deposition duration was controlled to be 30 min, and the resulted film thickness was about 0.7-1.2 μm.

2.2 Characterization

The phase structure of the films was analyzed using X-ray diffraction (XRD, Philips X′Pert Pro) with Cu Ka radiation (40 kV, 30 mA). The film morphology was observed by field emission scanning electron microscopy (FESEM, JSM-6701F) attached with an energy dispersive X-ray spectroscopy (EDS). The film nanostructure was observed by high-resolution transmission electron microscopy (HRTEM, Tecnai G2 F20S-Twin) operating at 200 kV. The sample for HRTEM analysis was prepared by a mechanical polishing method and then Ar ion milled at a low angle in regard to sample surface.

2.3 Friction tests

The ground-based atomic oxygen simulation system has been described elsewhere [21]. A microwave-electron convolute resonance power source was employed to produce oxygen plasma in the vacuum chamber assembled by a ball-on-disk tribometer. The formed positive oxygen ions plasma beam could be accelerated and neutralized with the negative charges on the polar plate with a negatively charged electric field to produce a neutral AO beam. The translational kinetic energy and flux of AO irradiation on WS_2 film surface could be controlled by changing the microwave power and base pressure of oxygen. In this ground-based simulation system, the vacuum condition, AO irradiation and friction test could be controlled by independent operating systems. The friction experiments were implemented using a home-made ball-on-disk tribometer equipped with an AO irradiation source in three different environments (vacuum, AO or vacuum/AO alternate environments). The disk was the WS_2 coated substrate, and the counterpart was the GCr 15 steel ball with a diameter of 3.175 mm and the surface roughness of 0.1 μm (Ra). During the sliding friction process, the ball was fixed and the disk was rotating in a fixed direction. For all the tests, the applied normal load was 2 N and the rotation speed was 100 r/min. For the vacuum friction, the base pressure was lower than 6×10^{-3} Pa. For the in-situ AO-irradiation friction test, the AO kinetic energy and flux at the sample surface

were controlled to be 5.0 eV and 2.5×10^{15} atoms·cm^{-2}·s^{-1}, respectively, and the ambient pressure was 3.5×10^{-2} Pa. For the in-situ AO irradiation/vacuum alternative environments, the cycle period and AO irradiation duty ratio were 120 s and 50 %, respectively. After the friction tests, the morphology and composition of the wear track and debris were analyzed by FESEM and X-ray photoelectron spectroscopy (XPS, PHI Quantera Scanning X-ray Microprobe) equipped with a monochromatic Al Ka X-ray source of 1486.6 eV (hν). All the XPS spectra were referenced with respect to C 1s peak at binding energy of 284.6 eV. The XPS PEAK 4.1 software was used for the deconvolution and fitting of the multiplex spectra using Gaussian function, in which the background of the spectra was subtracted using Shirley's method.

3. Results and discussion

3.1 Film structure

Generally, the sputtered WS_2 film exhibited a porous columnar microstructure with a worm-like or dendrite-like surface, and the wear resistance was not optimal due to this inferior microstructure [20]. In this study, the deposition processes of WS_2 films were carefully designed and controlled to obtain dense and loose film microstructures, respectively. **Fig. 1** shows the typical top view and cross-section SEM images of the dense WS_2 film. In comparison with the common porous columnar microstructure [21], this film was obviously densified. A columnar morphology was still observed but without the WS_2 micro-platelets and micro-pores. The XRD result (**Fig. 2**) revealed that this dense WS_2 film mainly exhibited 2H-WS_2 (002), (100) and (111) diffraction peaks with relatively broad peak shape. It implied that the growth of WS_2 micro-platelets was significantly suppressed during dense film growth process owing to the relatively strong plasma's bombardment at low argon pressure [22]. As a result, the self-shadow effect of WS_2 micro-platelets on growing film was weakened and the film microstructure became compact. HRTEM and SAED results (shown in **Fig. 3)** proved that the dense film was mainly composed of WS_2 nanocrystallites with a size of several nanometers, indicating that the crystallinity of the deposited dense WS_2 film was poor. This superior dense microstructure was expected to acquire the better wear resistance for the TMDs films [23].

3.2 Friction and wear behaviors

Fig. 4 shows the two friction curves of dense WS_2 films in the vacuum and AO environments, respectively. In the vacuum environment, the dense WS_2 film presented a stable and low friction behavior throughout the friction process of 2.3×10^4 cycles. The mean value of friction coefficient was 0.03. It should be pointed out that the attention was mainly paid to the in-situ AO-irradiation friction behavior of WS_2 film in this study so that the film friction test in a vacuum environment was not carried out to its wear life terminus. In the AO environment, the friction coefficient became relatively high and unstable, and it even showed sharp increase after the sliding friction reached to 1.1×10^3 cycles, indicating that the film was failed. The mean friction coefficient of dense WS_2 film was determined to be ~0.07 before the lubrication failure. Clearly, the in-situ AO-irradiation resulted in the detrimental effect on the tribological properties of WS_2 film: the wear life declined sharply from greater than 2.3×10^4 cycles to 1.1×10^3 cycles (the latter was only one twentieth of the former) and the friction coefficient skipped from 0.03 to 0.07. Previous studies [9-16] revealed that in the ex-situ experiments, the AO irradiation effect on the MoS_2 film was just reflected in the film surface oxidation and increase of friction coefficient in the initial friction stage. For example, Cross et al. [10] reported that the AO-irradiated MoS_2 film exhibited an initial high friction coefficient (up to 0.25), but it dropped to the normal

low value soon just after several sliding cycles. Similar results were also observed from our previous studies on the space-exposed MoS_2 based films [15, 16] and the ground AO-irradiated WS_2 film [24]. Unlikely, in this in-situ irradiation investigations, the high friction behavior was continuing throughout the friction process and the wear life decreased significantly as the degraded material on the upper surface was removed. Namely, the in-situ irradiation condition was much harsher than the ex-situ one.

There was no doubt that the oxidation of WS_2 films by the AO irradiation should be responsible for its high friction and low anti-wear behavior in the sliding friction process. Previous studies [9-12] have reported that in the ex-situ AO-irradiation experiment, the MoS_2 and WS_2 films surface could be rapidly oxidized to form an ultra-thin oxidation layer which could act as an effective protection layer inhibiting the further oxidation on the surface. These oxidation products of ex-situ AO-irradiated films, mainly MoO_3 for MoS_2 [16] and WO_3 for WS_2 [24], were without lubricity and the films always exhibited high friction only in the initial friction stage because the thin oxidation layers could be exfoliated quickly by the frictional interaction. In the in-situ AO irradiation conditions, the oxidation and high friction behavior of the WS_2 film occurred simultaneously. The instantly formed oxidation layer on the wear track of WS_2 film induced by in-situ AO irradiation would be exfoliated in layer-by-layer by the dynamic frictional interaction accompanying by the inevitable high friction and wear.

The FESEM images in **Figure 5** (a and b) exhibit the wear tracks of the dense WS_2 film after the sliding friction in the vacuum and AO irradiation environments, respectively. The morphology results suggested that there are many particle-like wear debris distributed along the sides of the wear track in the AO environment. Comparatively, the particle-like wear debris was less for the WS_2 film even after more sliding cycles in a vacuum environment. The further element composition analysis of wear track by XPS (listed in **Table 1**) revealed that the elements of W, S, O and C were detectable. Unsurprisingly, the high C content was present because it was normal in XPS analysis. It is worth noting that the difference in S/W atomic ratio was obvious for the wear tracks formed in both environments. For the dense WS_2 film, the S/W ratio (~1.5) on the wear track formed in vacuum was close to the value of the as-deposited WS_2 film (~1.7). However, the S/W ratio value reduced to ~0.9 after test under in-situ AO irradiation friction condition. Furthermore, the O concentration of 40 at.% in wear track was recorded after in-situ AO irradiation friction which was much higher than that of 26 at.% in vacuum. The above results of the morphologies and element composition of the wear tracks intensively indicated that the WS_2 film was oxidized and peeled away concurrently at the contact interface in the synchronous process of AO irradiation and sliding friction.

The friction contact zones of wear tracks formed in both environments (as shown in **Fig. 5**) were further analyzed by XPS and the XPS W 4f spectra are shown in **Fig. 6** (a) and (b). It is obviously that three peak profiles could be observed in both W 4f spectra but the relative intensities of them were very different. The lowest and highest binding energies were assigned to W (IV) $4f_{7/2}$ and W (VI) $4f_{5/2}$ being located at 32.8 and 37.8 eV, respectively. According to the position, area and full width at half maximum (FWHM) of both W(IV) $4f_{7/2}$ and W(VI) $4f_{7/2}$ peaks, the original middle peak was fitted to two peaks of W (IV) $4f_{5/2}$ at 35.0 eV and W (VI) $4f_{7/2}$ at 35.6 eV using a Gaussian function. The XPS W (VI) 4f peaks were identified to be WO_3 as a normal oxidation product of WS_2 [25], and the XPS W (IV) 4f peaks to the original state of WS_2 [26]. Referring to the W (IV) and (VI) peak areas, the relative concentrations for WO_3 and WS_2 were determined as showed in **Fig. 6**. For the wear track of dense WS_2 film formed under the vacuum friction, the ratio of WO_3 to

WS_2 was 37:63, indicating that the main composition was WS_2. On the contrary, the WO_3 was predominant in the wear track after the in-situ AO irradiation friction test of dense WS_2 film: up to 77 % of WO_3. These results further verified that in the synchronous process of AO irradiation and sliding friction, the wear of the WS_2 film was mainly controlled by the oxidation firstly and then exfoliation by friction interaction.

To further clarify the friction and wear behavior of the WS_2 films in the AO irradiation environments, the friction test in the vacuum/AO alternative environment was implemented and the typical friction curve is showed in **Fig. 7**. The dense WS_2 film show a significantly different friction behavior as the environmental was changed. Namely, the WS_2 film showed a high/unstable friction behavior in the AO-irradiation environment, but it dropped to a low/stable stage when the environment was switched into the moderate vacuum. The periodic process was repeated until the lubrication of film failed. In addition, it was worth noting that a transitional period of friction coefficients was also obviously observed when the environment was changed. The friction coefficient showed a gradually increasing trend when the environment was switched from a vacuum to AO, while it represented a sharp decrease as the environment was switched in the reverse process. The former transitional period of sliding friction was about 24 cycles, much longer than that of the latter (8 cycles). In the former stage, the wear track surface would reach a steady state gradually under the synergistic action of AO irradiation and friction, which was more dependent on the oxidation and the irradiation time of AO rather than the sliding revolutions. The latter stage was to eliminate the oxidation product effect on the friction, which virtually depended on how many friction revolutions were needed but not the friction time. Thus, it is believed that friction revolutions for transitional periods of friction coefficient from low to high values must be reduced if the friction tests were carried out with lower rotational speed, while in the other transitional period of friction coefficient from high to low value, the required revolutions to eliminate the oxidation product effect on the friction should be not varied significantly. Moreover, another noticeable phenomenon was that the friction coefficient underwent a "V-shaped" fluctuation in each revolution under the synchronous process of AO irradiation and sliding friction, as shown in inset of **Fig. 7**. The absence of this phenomenon in the vacuum friction process implies that the regular "V-shaped" fluctuation originated from the AO irradiation effect but not instrumental error of the tribometer. Further work is needed to fully understand it. Overall, the in-situ AO irradiation has a big negative influence on the tribological properties of the WS_2 films, which resulted in not only the increased friction coefficient and noise but also the significant deterioration in the wear resistance. The high friction and severe wear were related with the continuous formation of oxidation product by AO irradiation and exfoliation of these non-lubricious oxidation products by the frictional interaction.

It is well known that the WS_2 composite films always have better wear resistances and wider applications than the pure WS_2 film. The better wear resistances of WS_2 composite films were mainly attributed to their dense microstructure in comparison with that of pure WS_2 film [18-20]. It was noted that the WS_2 composite film was not taken into consideration in this study to avoid some conceivable covering effects of dopants on the response of WS_2 phase to active AO. Nevertheless, the microstructural effect on the in-situ AO irradiation friction and wear behavior of WS_2 films was further considered by comparatively investigating another loose structural WS_2 film. **Fig. 8** shows the friction curves of the loose WS_2 film in the vacuum and AO irradiation environments, respectively, in which the surface topography FESEM image of the loose WS_2 film was inserted in the top right corner. In comparison to the dense WS_2 film shown in **Fig. 1**(a), the loose WS_2 film exhibited a

porous microstructure and poor wear resistance in vacuum environment (wear life of 1.7×10^4 cycles). However, the wear lives of both loose and dense WS_2 films were almost equivalent (1.1×10^3 cycles) in the conditions of synchronous action of AO irradiation and friction. Similar to the dense WS_2 film, a plenty of particle-like wear debris was observed along the wear track for the loose WS_2 film after the in-situ AO irradiation friction process (**Fig. 9**), which clearly indicated that the severe wear of film occurred due to the oxidation and delamination.

In generally, the solid lubricant films with better wear resistance in vacuum environment also showed almost unchanged tribological properties even after the AO irradiation in the ex-situ condition [24]. The two WS_2 films with dense or loose structure presented a significant difference in the wear life in moderate vacuum due to the different microstructural compactness, but their wear lives in in-situ AO-irradiation friction process were almost identical in this study. It could be stated that the importance of film compactness for the wear resistance was different in both in-situ and ex-situ AO irradiation conditions. Thus, it would be unrealistic for the WS_2 and MoS_2-based films to significantly enhance their wear resistances in the ground simulation AO irradiation or real space exposure environments only by simply densifying their microstructure. To achieve a desired purpose, it was necessary to fundamentally improve the anti-oxidation ability of the WS_2 based films against the destructively synchronous action of AO irradiation and frictional interaction.

4. Conclusion

The pure WS_2 films with loose and dense microstructures were designed and prepared successfully by sputtering method, respectively. The loose microstructure was typical for pure TMDs film and the dense microstructure was normal for the WS_2 composite film. Being significantly different from the conventional ex-situ AO irradiation method, both WS_2 films exhibited a high/unstable friction and severe wear against the synchronization action of in-situ AO-irradiation and friction. The high and unstable friction mainly resulted from the formation of non-lubricating oxidation product (WO_3) on the wear track surface by active AO irradiation and thereby the rapid delamination of it by frictional interaction was responsible for the high wear behavior. Even though the wear resistance was different for the both loose and dense WS_2 films in the vacuum, the wear lives of them were almost identical poor value of 1.1×10^3 cycles in the in-situ AO-irradiation and friction condition. This clearly indicated the friction and wear behavior should be not dependent on the film compactness but on its anti-oxidation ability. The effective approach to significantly improve wear resistance of WS_2 film in the potential service condition should be to enhance its anti-oxidation ability rather than simply densify the film microstructure.

Acknowledgement

The authors are grateful for the financial support provided by China National Natural Science Foundation (Grant No. 51575508, 51505465, 51575509 and 51227804).

References

[1] K.L. Bedingfield, R.D. Leach, M.B. Alexander, NASA Reference Publication 1390, August 1996.

[2] E.M. Silverman, NASA Contractor Report 4661: Part 1, August 1995.

[3] H.G. Pippin, S.L.B. Woll, K.Y. Blohowiak, L.K. Olli, J.H. Osborne, Prog. Org. Coat. 47 (2003) 458-468.

[4] X.M. Gao, M. Hu, J.Y. Sun, Y.L. Fu, J. Yang, L.J. Weng, W.M. Liu, Appl. Surf. Sci. 320 (2014) 466-470.

[5] M. Tagawa, K. Yokota, Acta Astronaut. 62 (2008) 203-211.
[6] E.W. Roberts, M.J. Todd, Wear 136 (1990) 157-167.
[7] M. Hu, X.M. Gao, J.Y. Sun, L.J. Weng, F. Zhou, W.M. Liu, Appl. Surf. Sci. 258 (2012) 5683-5688.
[8] M. Tagawa, K. Yokota, K. Matsumoto, M. Suzuki, Y. Teraoka, A. Kitamura, M. Belin, J. Fontaine, J. Martin, Surf. Coat. Technol. 202 (2007) 1003-1010.
[9] J.A. Martin, J.B. Cross, L.E. Pope, Mat. Res. Soc. Symp. Proc. 140 (1989) 271-276.
[10] J.B. Cross, J.A. Martin, L.E. Pope, S.L. Koontz, Surf. Coat. Technol. 42 (1990) 41-48.
[11] M. Tagawa, K. Yokota, N. Ohmae, K. Matsumoto, M. Suzuki, Tribol. Lett. 17 (2004) 859-865.
[12] M. Arita, Y. Yasuda, K. Kishi, N. Ohmae, Tribol. Trans. 35 (1992) 374-380.
[13] M. Tosa, A. Kasahara, M. Goto, Y. Pihosh, E. Miyazaki, Y. Kimoto, M. Suzuki, K. Imagawa, T. Jpn. Soc. Aeronaut. S. 7 (2009) 63-66.
[14] M.T. Dugger, T.W. Scharf, S.V. Prasad, Adv. Mater. Pro. 172 (2014) 32-35.
[15] X.M. Gao, M. Hu, J.Y. Sun, Y.L. Fu, J. Yang, W.M. Liu, L.J. Weng, Appl. Surf. Sci. 330 (2015) 30-38.
[16] X.M. Gao, M. Hu, J.Y. Sun, Y.L. Fu, J. Yang, W.M. Liu, L.J. Weng, Vacuum 144 (2017) 72-79.
[17] B.A. Krick, W.G. Sawyer, Tribol. Lett. 41 (2011) 303-311.
[18] P. Mutafov, M. Evaristo, A. Cavaleiro, T. Polcar, Surf. Coat. Technol. 261 (2015) 7-14.
[19] S.S. Xu, X.M. Gao, M. Hu, J.Y. Sun, D. Jiang, F. Zhou, W.M. Liu, L.J. Weng, Appl. Surf. Sci. 288 (2014) 15-25.
[20] T.W. Scharf, A. Rajendran, R. Banerjee, F. Sequeda, Thin Solid Films 517 (2009) 5666-5675.
[21] S.S. Xu, X.M. Gao, M. Hu, D.S. Wang, D. Jiang, J.Y. Sun, F. Zhou, L.J. Weng, W.M. Liu, Tribol. Lett. 55 (2014) 1-13.
[22] A. Anders, Thin Solid Films 518 (2010) 4087-4090.
[23] M.C. Simmond, A. Savan, E. Pflüger, H. Van Swygenhoven, Surf. Coat. Technol. 126 (2000) 15-24.
[24] S.S. Xu, X.M. Gao, M. Hua, J.Y. Sun, D. Jiang, D.S Wang, F. Zhou, L.J. Weng, W.M. Liu, Appl. Surf. Sci. 298 (2014) 36-43.
[25] A.P. Shpak, A.M. Korduban, M.M. Medvedskij, V.O. Kandyba, J. Electron. Spectrosc. Relat. Phenom. 156-158 (2007) 172-175.
[26] X.B. Xie, R.E. Mccarley, Inorg. Chem. 34 (1995) 6124-6129.

Figures and Tables captions

Fig. 1. SEM micrographs of the dense WS_2 film: (a) surface and (b) cross-section.

Fig. 2. XRD pattern of the deposited dense WS_2 film.

Fig. 3. (a) Cross-sectional HRTEM micrograph and (b) SAED pattern of the dense WS_2 film.

Fig. 4. Typical friction curves of the dense WS_2 film in vacuum and AO environments.

Fig. 5. FESEM images of the wear tracks for the dense WS_2 films after the sliding friction in different environments: (a) vacuum and (b) AO irradiation.

Fig. 6. XPS W 4f spectra obtained from the wear tracks for the dense WS_2 films after the vacuum and in-situ AO irradiation friction.

Fig. 7. Friction curve of the dense WS_2 film in the vacuum/AO alternate environment.

Fig. 8. Friction curves of the loose WS_2 film in the vacuum and in-situ AO irradiation environments.

Fig. 9. SEM image for the wear track of loose WS_2 film after the in-situ AO irradiation friction.

Table 1. Atomic concentrations of the wear track analyzed by XPS for the WS_2 films after the friction in the vacuum and AO irradiation environments.

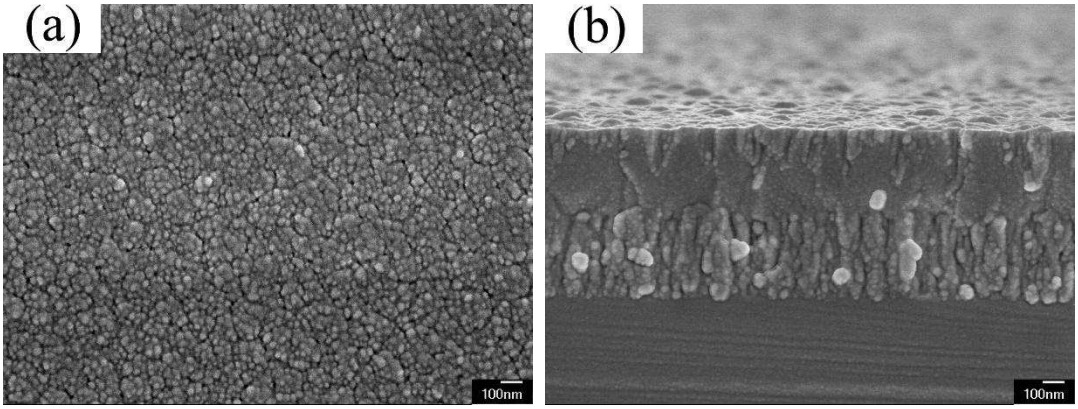

Fig. 1

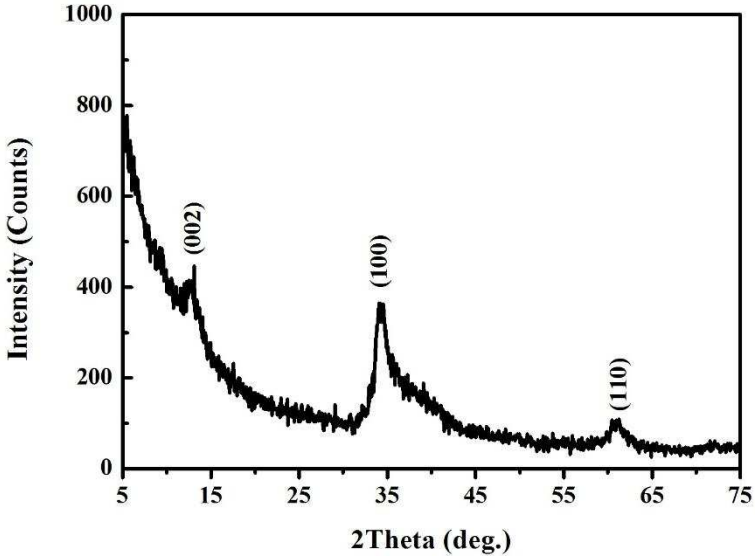
Intensity (Counts)
1000
800
600
400
200
0
(002)
(100)
(110)
5
15
25
35
45
55
65
75
2Theta (deg.)

Fig. 2

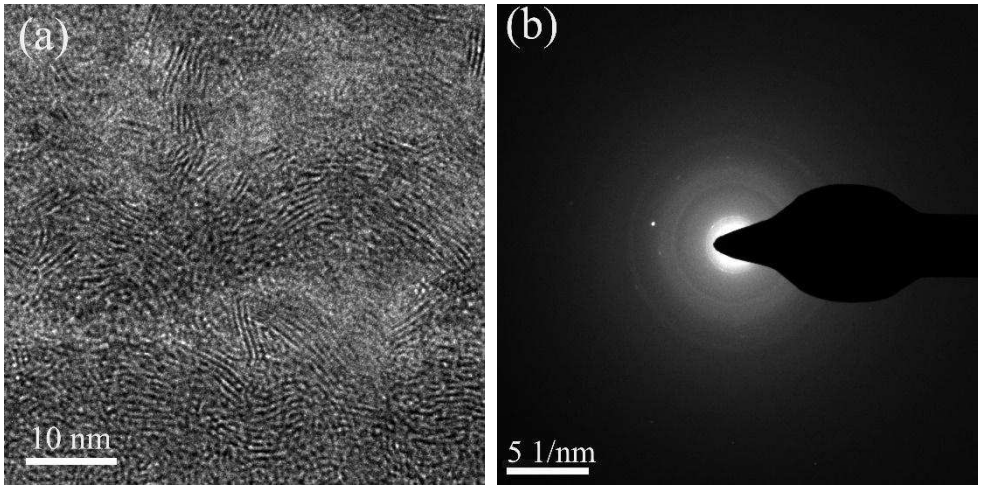

Fig. 3

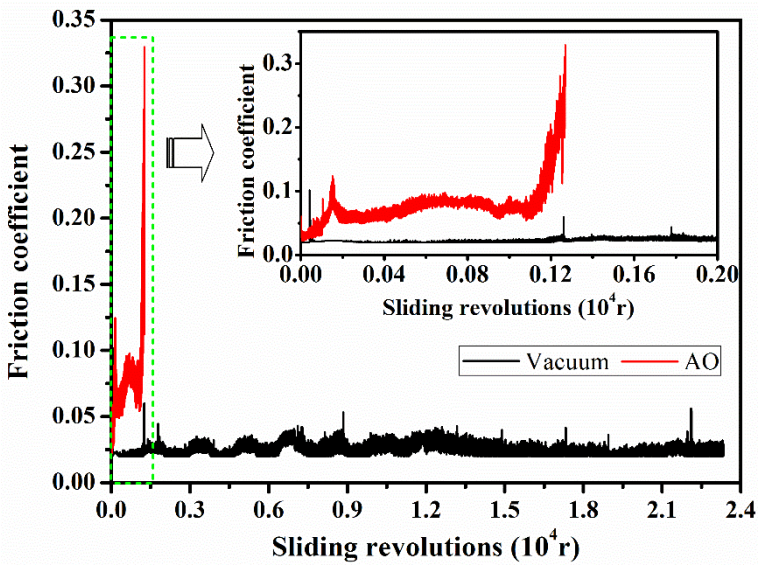
Friction coefficient
Sliding revolutions (10^4r)
Vacuum
AO
0.35
0.30
0.25
0.20
0.15
0.10
0.05
0.00
0.0
0.3
0.6
0.9
1.2
1.5
1.8
2.1
2.4
0.3
0.2
0.1
0.0
0.00
0.04
0.08
0.12
0.16
0.20

Fig. 4

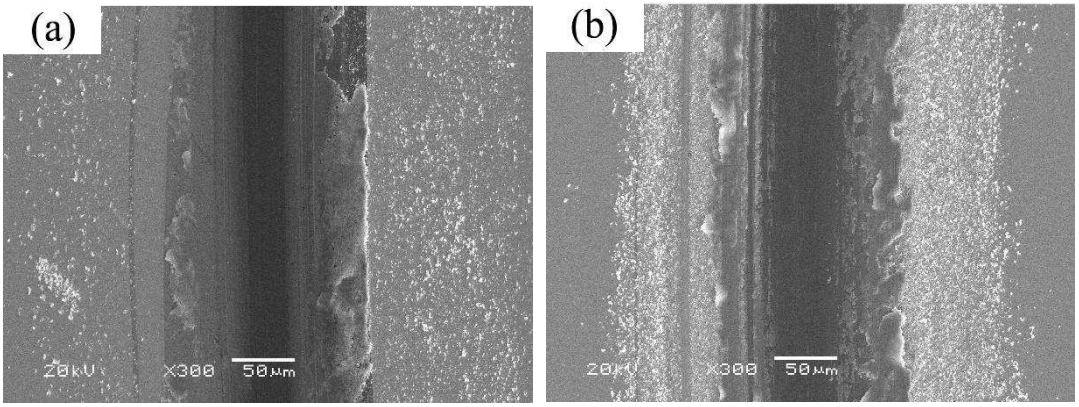

Fig. 5

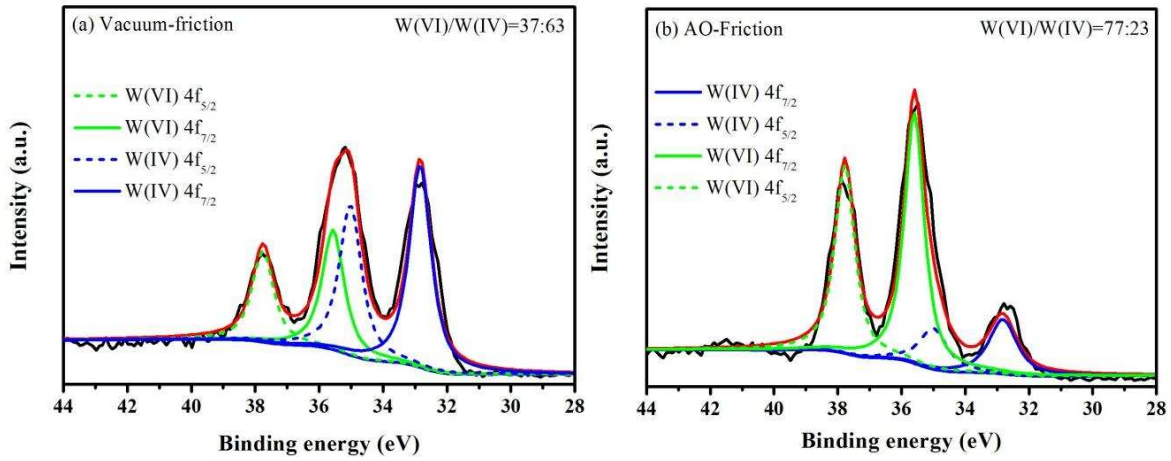
(a) Vacuum-friction
W(VI)/W(IV)=37:63
W(VI) 4f5/2
W(VI) 4f7/2
W(IV) 4f5/2
W(IV) 4f7/2
Intensity (a.u.)
Binding energy (eV)
(b) AO-Friction
W(VI)/W(IV)=77:23
W(IV) 4f7/2
W(IV) 4f5/2
W(VI) 4f7/2
W(VI) 4f5/2
Intensity (a.u.)
Binding energy (eV)

Fig. 6

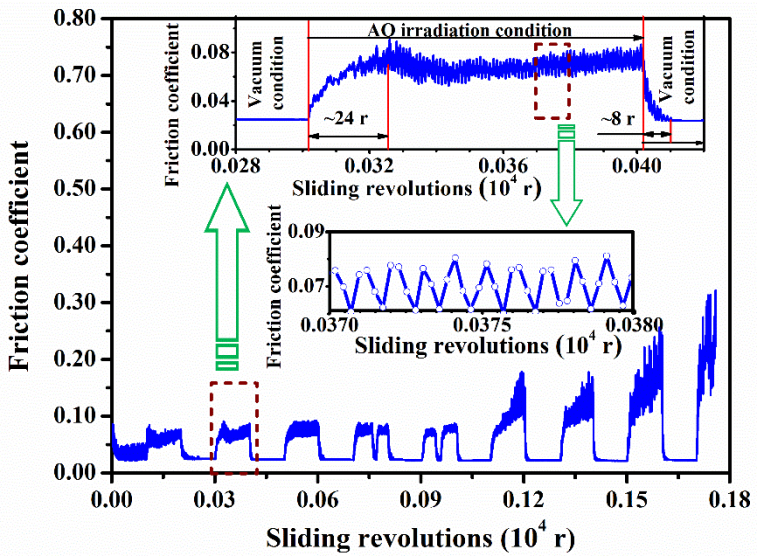
Friction coefficient
Sliding revolutions (10^4 r)
Vacuum condition
AO irradiation condition
Vacuum condition
~24 r
~8 r
Friction coefficient
Sliding revolutions (10^4 r)

Fig. 7

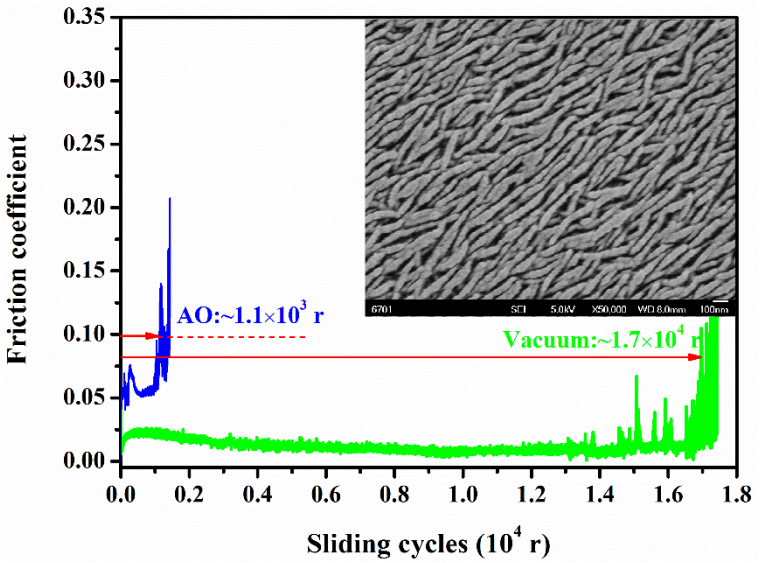
Friction coefficient
0.35
0.30
0.25
0.20
0.15
0.10
0.05
0.00
0.0
0.2
0.4
0.6
0.8
1.0
1.2
1.4
1.6
1.8
Sliding cycles (10^4 r)
AO:~1.1×10^3 r
Vacuum:~1.7×10^4 r

Fig. 8

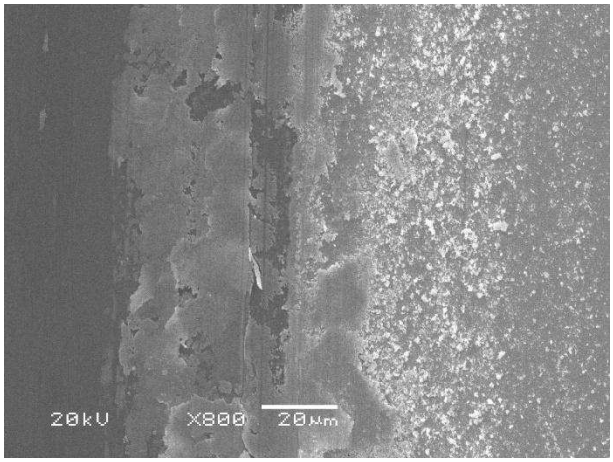

Fig. 9

Table 1

Samples	Atomic concentration (%)				S/W ratio
	C	W	S	O	
Vacuum	49	10	15	26	1.5
AO irradiation	39	11	10	40	0.9